

# Barrier Layer Effect of Tantalum on the Electromigration in Sputtered Copper Films on Hydrogen Silsesquioxane and SiO<sub>2</sub>

WEN-LI SUNG and BI-SHIOU CHIOU

Department of Electronics Engineering and Institute of Electronics, National Chiao Tung University, Hsinchu, Taiwan

As IC devices scale down to the submicron level, the resistance-capacitance (RC) time delays are the limitation to circuit speed. A solution is to use low dielectric constant materials and low resistivity materials. In this work, the influence of underlying barrier Ta on the electromigration (EM) of Cu on hydrogen silsesquioxane (HSQ) and SiO<sub>2</sub> substrates was investigated. The presence of a Ta barrier not only improves the adhesion between Cu and dielectrics, but also enhances the crystallinity of Cu film and improves the Cu electromigration resistance. The activation energy obtained suggests a grain boundary migration mechanism and the current exponent calculated indicates the Joule heating effect.

**Key words:** Cu-low k dielectric, electromigration, barrier layer, metallization reliability

## INTRODUCTION

As interconnect feature size decreases and clock frequencies increase, the on-chip resistance-capacitance (RC) time delays become the major limitation in achieving faster circuit speeds. In order to reduce the time delays, the use of low-resistivity and low dielectric constant materials is a way to limit the interconnect RC time delays for ULSI metallizations.

Copper is the most attractive interconnect for future devices because Cu has an electrical bulk resistivity of 1.7  $\mu\Omega$  cm and better electromigration resistance compared with aluminum alloys.<sup>1</sup> However, the use of copper has some challenges, such as the lack of a stable self-passivating copper oxide, poor adhesion to dielectric materials, and diffusion of Cu into substrates.<sup>2-4</sup> Therefore, the use of diffusion barriers between Cu and the underlying substrate is required.<sup>5-7</sup> Hydrogen silsesquioxane (HSQ), with the general formula (HSiO<sub>3/2</sub>)<sub>2n</sub>, n = 2, 3, 4 . . . etc.,<sup>8,9</sup> has many advantages such as low dielectric constant (k about 2.7), carbon-free, nonetchback processing, excellent gap-filling, good planarization, and low moisture uptake, and is a potential low k material for ULSI application.

Tantalum is an attractive barrier metal in many applications because of its good electrical conductivity, high melting point, and chemical inertness.<sup>10</sup> It was reported that a Ta barrier layer prevented the

diffusion of Cu into Si substrates<sup>11</sup> and affected the texture and grain size of deposited Cu, which are critical factors in determining electromigration reliability.<sup>5,11</sup>

In this work, the influence of an underlying barrier Ta on the electromigration of Cu deposited on HSQ and SiO<sub>2</sub> substrates was investigated. The kinetics of electromigration damage (EMD) are studied by an isothermal resistance change analysis method using the empirical formula<sup>2,12,13</sup>

$$dR/dt * 1/R_0 = AJ^n \exp(-Q/kT) \quad (1)$$

The activation energy Q for EMD and the exponent n of the current density are calculated and discussed.

## EXPERIMENTAL PROCEDURES

Four-inch diameter p-type (100) Si wafers with nominal resistivity of 1–10  $\Omega$  cm were used as substrates. After standard RCA cleaning, 50 nm thermal oxide was grown at 950°C in a steam atmosphere on some Si substrates. Hydrogen silsesquioxane (HSQ) was prepared by spin-coating Dow Corning Flowable Oxide (FOX-15) on the cleaned Si wafer. The dispense-and-spread cycle was carried out at 500 rpm for 5 sec, and the final ramp cycle was 2000 rpm for 20 sec. The wafers were baked sequentially at 150°C, 200°C, and 300°C for 1 min each on three hot plates.

(Received November 1, 2001; accepted January 8, 2002)

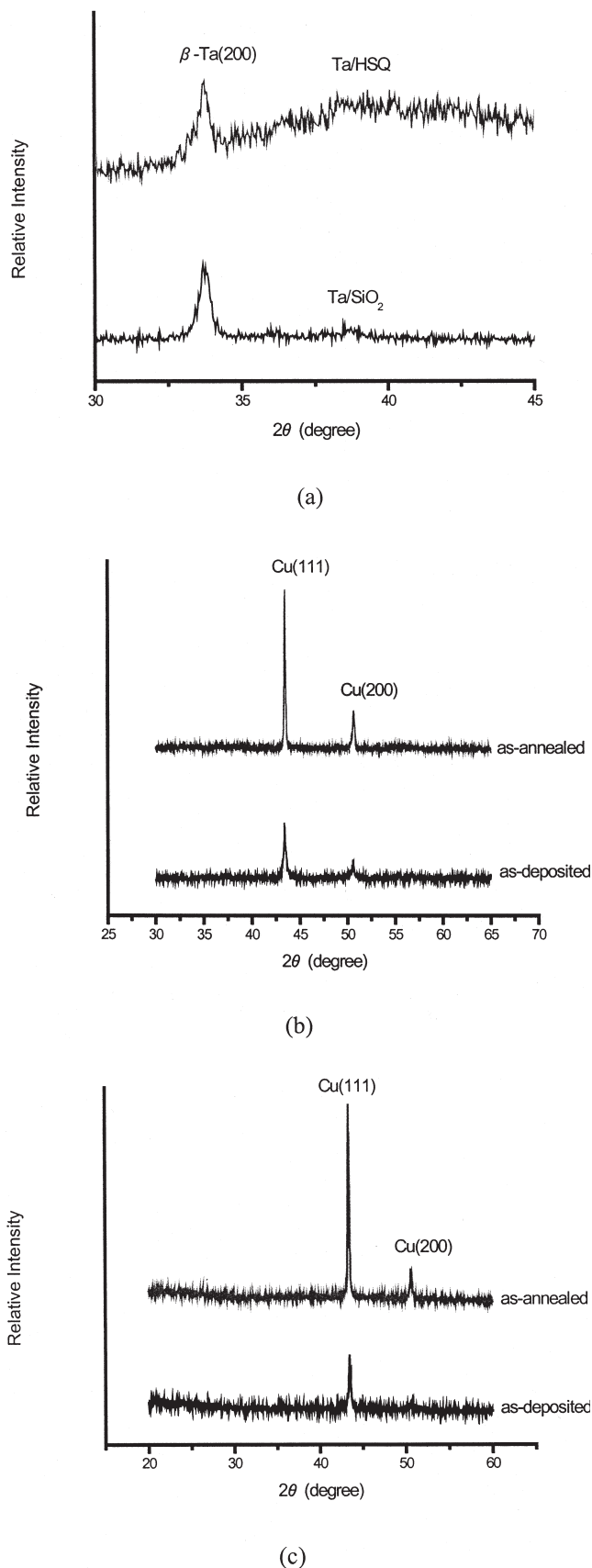


Fig. 1. The XRD patterns of (a) Ta film on SiO<sub>2</sub> and HSQ substrates, (b) Cu/Ta films on SiO<sub>2</sub>, and (c) Cu/Ta films on HSQ. Annealing condition: 400°C for 1 h.

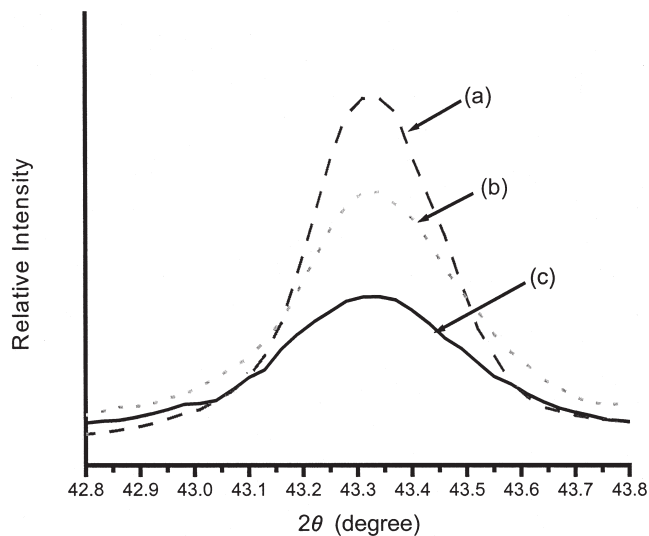


Fig. 2. The Cu (111) peak of (a) Cu/Ta/SiO<sub>2</sub>/Si, (b) Cu/Ta/HSQ/Si, and (c) Cu/SiO<sub>2</sub>/Si.

Curing (completely imidized) HSQ was performed in an N<sub>2</sub> furnace at 400°C for 1 h. The cured thickness of HSQ was about 650 nm. Both the SiO<sub>2</sub>-coated and HSQ-coated Si substrates were then processed with conventional photolithography to obtain a test pattern. Samples with positive photore-

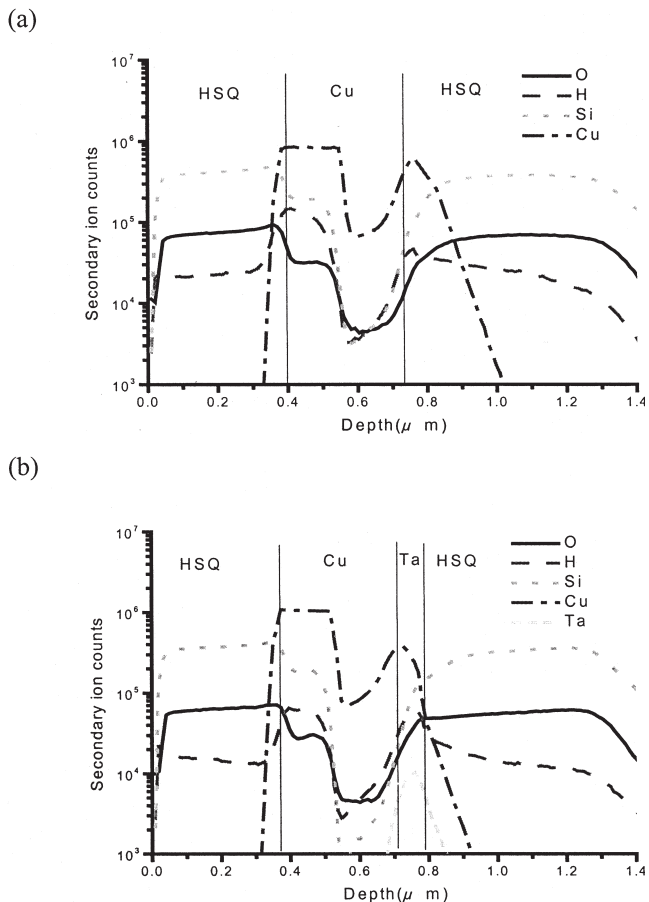


Fig. 3. The SIMS depth profiles of (a) HSQ/Cu/HSQ/Si structure and (b) HSQ/Cu/Ta/HSQ/Si structure, both annealed at 400°C for 1 h.

sist patterns were transferred to a vacuum chamber for the sputtering of Ta and Cu films.

High-purity Ar gas was introduced through a mass flow controller after the vacuum chamber was evacuated to about  $10^{-6}$  torr. The flow rate of argon was 24 sccm. The sputtering targets were 99.99% Cu disc and 99.95% Ta disc. Before deposition, the target was presputtered for 10 min to remove any contaminate. The gas pressure was kept at  $7.6 \times 10^{-3}$  torr and the sputtering power employed during deposition was 150 W for Ta and 200 W for Cu. The deposition rates are 0.03 nm/s and 0.14 nm/s for Ta and Cu, respectively. Copper film was sputtered after Ta deposition without breaking the vacuum. The film thicknesses were 300 nm copper and 10 nm Ta. The lift-off process was carried out after the sputtering of Ta and Cu to pattern for the EMD test. TEOS films, deposited by the decomposition of tetraethyl orthosilicate, 500 nm in thickness, were deposited onto Cu films with PECVD at 250°C and 100 mtorr.

Conventional photolithography was used to define the contact hole through the TEOS  $\text{SiO}_2$ . Blanket Al was then deposited on the specimen for the EM test by thermal coater, which was followed by photolithography. The solution of  $\text{H}_3\text{PO}_4:\text{HNO}_3:\text{CH}_3\text{COOH}:\text{H}_2\text{O} = 50:2:10:9$  was used to etch excess Al. Samples were then annealed in  $\text{N}_2$  ambient at 400°C for 1 h.

X-ray diffraction (XRD) was used to examine the metal films phase structure. A field emission scanning electron microscope was used to observe the surface morphology and microstructure. An atomic force microscope was employed to measure the surface morphology and roughness. A secondary ion mass spectrometer (SIMS) was employed to analyze elemental depth profiles.

The adhesion strength of Cu deposited on HSQ is evaluated with a direct pull tester. A stud was bonded perpendicularly to the coating surface with epoxy by holding it in contact through a spring mounting chip designed especially for the stud. The assembly was cured at 150°C for 1 h. The tester pulled the stud and samples down against the platen support ridge until the coating failed. The stress of adhesion,  $\sigma_a$  ( $\text{kg}/\text{mm}^2$ ), is defined as  $\sigma_a = F/A$ . The area of A is the circular section of the stud.

The electromigration tests were carried out in a quartz tube at temperatures ranging from 200°C to 300°C in air atmosphere. The four I/O pads of the samples were connected to a constant current source and a microvoltage meter.

## RESULTS AND DISCUSSION

The XRD patterns are shown in Fig. 1. There is no new compound formation detected in the XRD patterns. The  $\beta$ -Ta (200) peak ( $2\theta \sim 33.7^\circ$ ) is not visible after the deposition of Cu films. On  $\beta$ -Ta, the growth of Cu (111) is preferred. A comparison of the Cu (111) peak ( $2\theta \sim 43.3^\circ$ ) among the Cu film on  $\text{SiO}_2$ , Cu/Ta film on  $\text{SiO}_2$ , and Cu/Ta film on HSQ, shown

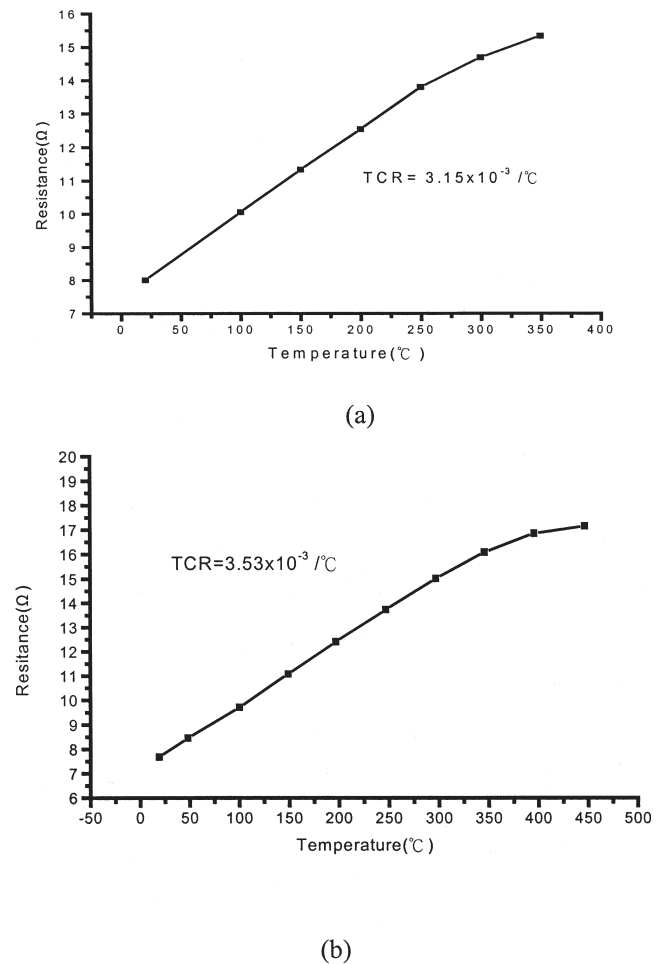
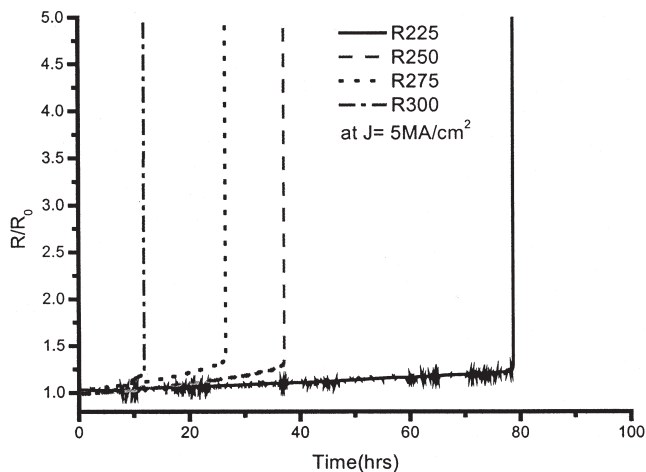


Fig. 4. Resistance of Cu/Ta films on (a) HSQ and (b)  $\text{SiO}_2$  as a function of temperature.  $\text{TCR} = \frac{1}{R_0} \frac{R - R_0}{T - T_0}$

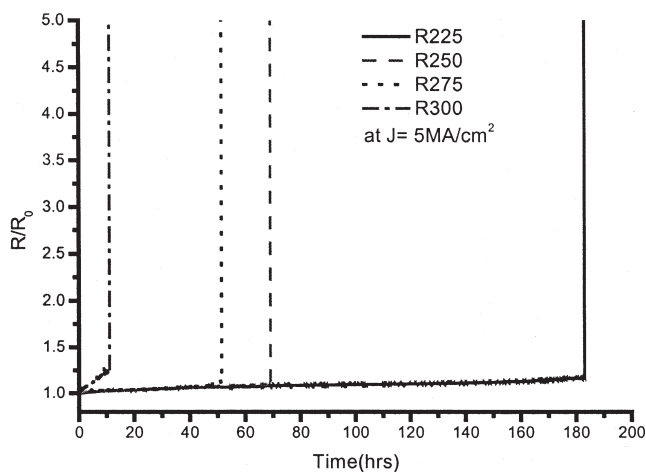
in Fig. 2, suggests that the presence of the Ta interlayer improves the crystallinity of Cu film. The degree of crystallinity of Cu/Ta on  $\text{SiO}_2$  is better than that of Cu/Ta on HSQ. The scanning electron microscopy microstructure does not reveal any apparent difference between the surface morphologies of Cu and Cu/Ta films.

The SIMS depth profiles of the HSQ passivated Cu/HSQ and Cu/Ta/HSQ specimens are shown in Fig. 3. On the Ta side of the Ta/HSQ interface, a decrease in the Si and O concentrations is observed. Nevertheless, the Ta side of the Ta/HSQ interface has a larger concentration of H than does the HSQ side of the Ta/HSQ interface. The H may have been dissociated from HSQ after annealing<sup>14</sup> and trapped in the Ta film. The H atoms behave as electron scatterers and the incorporation of H into Ta may raise the resistivity of the Ta film.

The film thicknesses of Ta and Cu are  $\sim 10$  nm and  $\sim 300$  nm, respectively. The resistivity of Ta is larger than that of Cu. Hence, current flow through the Ta film is negligible. The resistivities of Cu on  $\text{SiO}_2$  and Cu/Ta on HSQ are  $2.25 \pm 0.02 \mu\Omega \text{ cm}$  and  $2.26 \pm 0.07 \mu\Omega \text{ cm}$ , respectively. The presence of the



(a)



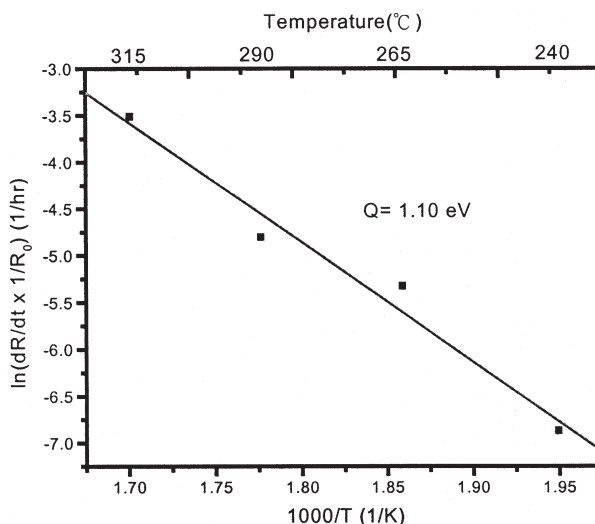
(b)

Fig. 5. The EMD tests of Cu/Ta films on (a) HSQ and (b) SiO<sub>2</sub> at a current density  $J = 5 \text{ MA/cm}^2$  at various testing temperatures.

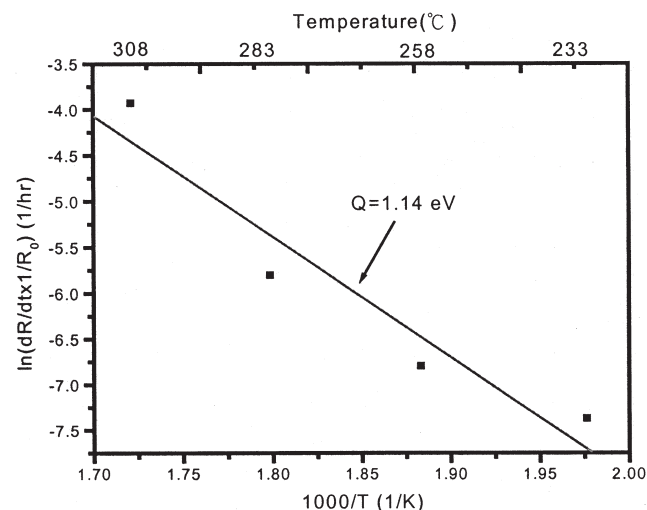
Ta interlayer does not affect the resistivity of the metallization.

On the basis of the SIMS spectra, it is not clear whether 10 nm of Ta film can effectively retard the diffusion of the Cu into the substrate. However, the presence of Ta does improve the adhesion of Cu to substrates. The adhesion strengths of the Cu/SiO<sub>2</sub> and Cu/HSQ interfaces are  $1.42 \pm 0.25 \text{ kg/mm}^2$  and  $6.97 \pm 1.87 \text{ kg/mm}^2$ , respectively. The presence of Ta raises the adhesion strength to  $31.35 \pm 3.24 \text{ kg/mm}^2$  (for Cu/Ta/SiO<sub>2</sub>) and  $16.81 \pm 5.01 \text{ kg/mm}^2$  (for Cu/Ta/HSQ). Addition of the Ta interlayer greatly enhances the adhesion strength of the interface. It is argued that the enhanced adhesion is due to the heteroepitaxial growth of Cu on  $\beta$ -Ta and the formation of a thin amorphous layer at the Ta/Cu interface.<sup>7,15</sup>

Since the resistance of metal varies in proportion to temperature, i.e.,  $R_2 = \alpha(T_2 - T_1) + R_1$ , the interconnect temperature can be monitored by measur-



(a)

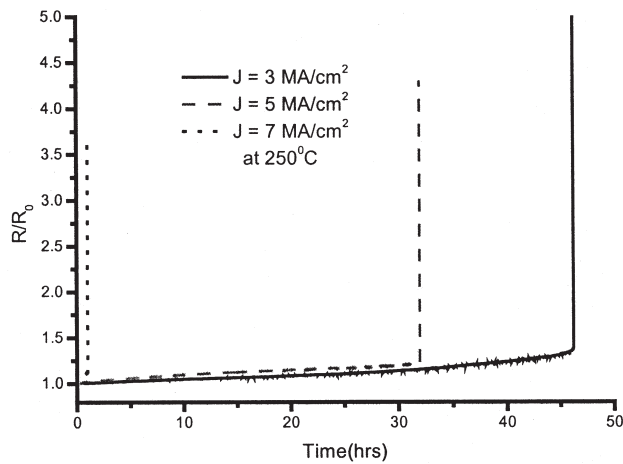


(b)

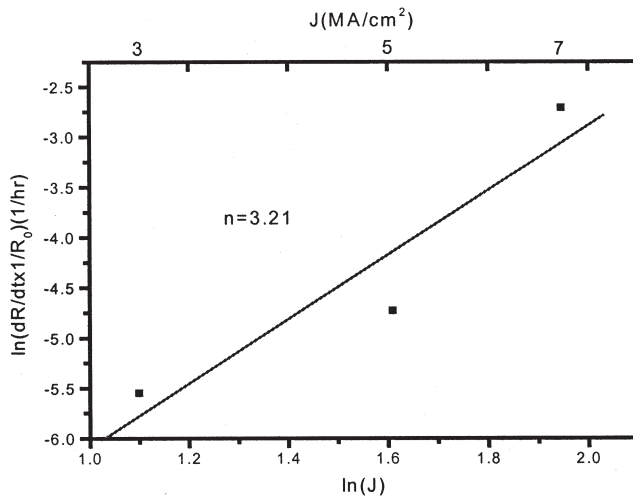
Fig. 6. The  $\ln[(dR/dt)(1/R_0)]$  vs.  $1/T$  for Cu/Ta films on (a) HSQ and (b) SiO<sub>2</sub> during EMD test. Current density:  $5 \text{ MA/cm}^2$ .

ing the resistance of a test metallization.<sup>16</sup> Figure 4 gives the resistance of Cu/Ta films on HSQ- and SiO<sub>2</sub>-coated Si substrates as a function of temperature. During the EMD experiment, the sample temperature is obtained from the measured resistance of the test metallization. The relative resistance  $R/R_0$  as a function of time at various temperatures is shown in Fig. 5. The resistance increases more rapidly at higher temperatures. By defining a resistance change of 4.5% as the criterion of early stage failure, i.e., assuming the dimensions of the maximum voids are much less than the line width, the time rate change of electrical resistance  $dR/dt$  due to electromigration damage is thermally activated and can be expressed by the following empirical equation:

$$dR/dt * 1/R_0 = AJ^n \exp(-Q/kT) \quad (1)$$



(a)



(b)

Fig. 7. (a) The EMD test of Cu/Ta films on HSQ at 250°C and various current densities and (b)  $\ln [(dR/dt)/(1/R_0)]$  vs.  $\ln J$  during the EMD test. Temperature: 250°C.

where  $R_0$  is the initial resistance at a given temperature,  $A$  is a pre-exponential factor,  $J^n$  is the electron current density raised to the  $n$ th power,  $T$  is temperature, and  $Q$  is the activation energy for EMD. The activation energies are obtained from the  $\ln [(dR/dt)/(1/R_0)]$  vs.  $1/T$  plot shown in Fig. 6 and are 1.1 eV and 1.14 eV for Cu/Ta films on HSQ and  $\text{SiO}_2$ , respectively. Hummel et al. reported that the activation energy for lattice migration in Cu is of the order of 2.3 eV, while that for grain boundary diffusion is about 1.2 eV.<sup>17</sup> The activation energies obtained suggest that lattices are not the major paths for electromigration in Cu/Ta. Migration via grain boundaries may play an important role in Cu/Ta, because the activation energy for the electromigration of Cu is 0.77 eV.<sup>4</sup> The Ta barrier layer enhances the migration resistance of copper.

Although the activation energies for the electromigration of Cu/Ta on HSQ and on  $\text{SiO}_2$  are similar, Cu/Ta films on  $\text{SiO}_2$  have longer EM lifetimes than do those on HSQ, as shown in Fig. 5. Dissociation of H from HSQ, as evidenced from the SIMS depth profile shown in Fig. 3, and diffusion of the impurity H into the Cu film may have changed the resistivity of the Cu (i.e., Poisson effect) and, consequently, resulted in shorter EM lifetime.<sup>5</sup> The relative resistance as a function of stress time at various temperatures is shown in Fig. 7a, and the current exponent  $n$  in Eq. 1, calculated from the EMD data, is 3.21. A current exponent of 2 has been obtained by solving a relatively simple diffusion equation where mass transport due to both concentration gradient and electromigration force are treated concurrently.<sup>7</sup> Values of  $n$  greater than 2 can probably be attributed to Joule heating effects, which result in a temperature gradient-induced flux divergence.

## CONCLUSIONS

The barrier effect of Ta on the electromigration of Cu film was investigated. The presence of an  $\sim 10$ -nm thick Ta interlayer enhances the adhesion strength of Cu/HSQ and Cu/ $\text{SiO}_2$  interfaces, although the effectiveness in blocking the diffusion of Cu into dielectric is not evident. The activation energies for electromigration failure are 1.10 eV and 1.14 eV for Cu/Ta films on HSQ and  $\text{SiO}_2$ , respectively, and suggest a grain boundary diffusion mechanism. Although no appreciable difference in activation energy is observed, Cu/Ta films on HSQ show shorter EM lifetimes than do those on  $\text{SiO}_2$ . Poisoning of metallization with hydrogen dissociated from HSQ increases the resistivity of Cu and results in the shorter EM lifetime of specimens on HSQ.

## ACKNOWLEDGEMENT

This work is sponsored by the National Science Council, Taiwan, under Contract No. 88-2216-EO09-012.

## REFERENCES

1. T. Nitta, T. Ohmi, T. Takewaki, and T. Shibata, *J. Electrochem. Soc.* 139, 992 (1992).
2. C.K. Hu, B. Luther, F.B. Kaufman, F. Hummel, C. Uzoh, and D.J. Pearson, *Thin Solid Films* 262, 84 (1995).
3. Y.L. Chin, B.S. Chiou, and W.F. Wu, *Jpn. J. Appl. Phys.* 39, 6708 (2000).
4. H.W. Wang, B.S. Chiou, and J.S. Jiang, *J. Mater. Sci.: Mater. Electron.* 10, 267 (1999).
5. H.Y. Hung and B.S. Chiou, *J. Electron. Mater.* (in press).
6. H.W. Wang and B.S. Chiou, *J. Mater. Sci.: Mater. Electron.* 11, 17 (2000).
7. C. Ryu, H. Lee, K.-W. Kwon, A.L.S. Loke, and S.S. Wong, *Solid State Technol.* 42, 53 (1999).
8. P.T. Liu, T.C. Chang, Y.L. Yang, Y.F. Chang, F.Y. Shih, J.K. Lee, E. Tsai, and S.M. Sze, *Jpn. J. Appl. Phys.* 38, 6247 (1999).
9. M.J. Loboda and G.A. Toskey, *Solid State Technol.* 41, 99 (1998).
10. J.C. Chuang and M.C. Chen, *Thin Solid Films* 332, 213 (1998).
11. T. Takewaki, H. Yamada, T. Shibata, T. Ohmi, and T. Nitta, *Mater. Chem. Phys.* 41, 182 (1995).



12. R. Rosenberg and L. Berenbaum, *Appl. Phys. Lett.* 12, 201 (1968).
13. M. Shatzkes and J.R. Lloyd, *J. Appl. Phys.* 59, 3890 (1986).
14. M.G. Albrecht and C. Blanchette, *J. Electrochem. Soc.* 145, 4019 (1998).
15. K.W. Kwon, C. Ryu, and R. Sinclair, *Appl. Phys. Lett.* 71, 3069 (1997).
16. T. Nitta, I. Ohmi, I. Hsohi, S. Sakai, K. Sakaibara, S. Imai, and T. Shibata, *J. Electrochem. Soc.* 140, 1131 (1993).
17. R.E. Hummel, R.T. Dehoff, and H.J. Geier, *J. Phys. Chem. Solids* 37, 73 (1976).